IMPACT LOADING BEHAVIOUR OF LARGE-SCALE TWO-WAY SANDWICH PANELS WITH NATURAL FIBRE-REINFORCED POLYMER FACES

Dillon Betts[1], Pedram Sadeghian[2*], and Amir Fam[3]

[1] Former PhD Student, Department of Civil and Resource Engineering, Dalhousie University, 5268 DaCosta Row, Halifax, NS B3H 4R2, Canada.

[2] Associate Professor and Canada Research Chair in Sustainable Infrastructure, Department of Civil and Resource Engineering, Dalhousie University, 5268 DaCosta Row, Halifax, NS, B3H 4R2, Canada.

[3] Donald and Sarah Munro Chair Professor in Engineering and Applied Science and Associate Dean (Research), Department of Civil Engineering, Queen's University, Kingston, ON, K7L 3N6, Canada.

** Corresponding author, email: pedram.sadeghian@dal.ca*

ABSTRACT: This paper presents experimental and numerical studies on sandwich panels with flax fiber-reinforced polymer (FFRP) faces and polyisocyanurate (PIR) foam cores. The panels are subjected to two-way bending under impact loads at the center, simulating applications like building cladding systems exposed to wind-borne debris. Nine large scale panels were fabricated and subjected impact loads; a total of 412 tests were performed. Each panel was 1220 mm by 1220 mm with a nominal thickness of 80 mm. The main test parameters were core-to-face thickness ratio based on one, two or three FFRP layers (core-to-face thickness ratio of 65.1, 32.6 and 21.7) and impact energy (50%, 70% and 95% of failure energy). For each face thickness, three identical panels were fabricated and tested. The impact tests were performed using a 140 mm diameter

drop weight ranging from 10.5 kg to 20 kg, with a varying height up to 3250 mm. The results showed that the panels are susceptible to internal damage accumulating after impacts, such as core shear failure. Analyses of the test data showed that impulse duration of a panel increased with an increase of damage. A finite element model was also developed to predict the behaviour of these panels under low energy impacts. The model accounts for the nonlinear behaviour of both the FFRP faces and foam cores. The model was used to perform a parametric study to examine the effect of core thickness, face thickness, and core density. It showed that impulse duration and maximum deflection increased with a decrease in face thickness, core density and core thickness.

DOI: https://doi.org/10.1061/JCCOF2.CCENG-4387

KEYWORDS: Sandwich Structures, Natural Fibers, Flax, Impact, Two-way, Impact

INTRODUCTION

Sandwich panels are structural members comprised of two stiff faces and a weaker lightweight core that separates the faces, providing a relatively large moment of inertia. These panels are ideal for light structural applications requiring a relatively high strength and stiffness. They are often made using fiber-reinforced polymer (FRP) faces and foam cores, in which case the panels provide dual benefits, namely thermal insulation and structural strength. Foam cores are relatively weak when compared to traditional FRPs such as carbon FRP (CFRP) or glass FRP (GFRP) and therefore the core typically controls the failure of the panel. In this case, the strength of the FRP skins may not be fully utilized. This presents an opportunity to replace the synthetic FRPs with more sustainable but lower strength natural FRPs (Mak et al. 2015; CoDyre et al.

2018; Sadeghian et al. 2018; Betts et al. 2018 and 2020). The behaviour of plant-based FRPs, such as flax FRPs (FFRPs) and hemp FRPs, have been studied extensively in the recent literature (Bensadoun et al. 2025; Christian et al. 2011; Baley et al. 2011; Sparnins 2006; Mak et al. 2019; Hristozov et al. 2016; Yan et al. 2016; Bambach 2017; Ramesh et al. 2017). FFRPs have been shown to have a lower embodied energy than both GFRPs and CFRPs (Cicala et al. 2010) and have a relatively high strength and stiffness when compared to other natural FRPs (Ramesh et al. 2017).

As building cladding systems can be exposed to high wind events, it is necessary to understand the behaviour of sandwich panels under both flexural and shear loading under wind and impact loads due to flying debris. Sandwich structures with synthetic faces have been investigated extensively under flexural loads (Sharaf et al. 2010; Gupta et al. 2002; Petras and Sutcliffe 1999; Manalo et al. 2016; Besant et al. 2001; Manalo et al. 2010; Dai and Hahn 2003; Fam and Sharaf 2010) and impact loads (Abrate 1997; Torre and Kenny 2000; Akil Hazizan and Cantwell 2002; Daniel et al. 2012), but in one-way bending. Also, sandwich structures with FFRP faces and cardboard cores (Betts et al. 2020; McCracken and Sadeghian 2018), paper honeycomb cores (Fu and Sadeghian 2020), and foam cores (Mak et al. 2015; CoDyre et al. 2018; Betts et al. 2018) have been investigated under one-way flexural and shear loads and under impact loads (Betts et al. 2020 and 2021).

Depending on the structural or architectural design, sandwich panels used for cladding materials can also be loaded in two-way bending. There has been substantial research on the two-way flexural (Dawood et al. 2009; Qi et al. 2016; Huo et al. 2015;

Satasivam et al. 2018) and impact behaviour (Schubel et al. 2004 ; Anderson and Madenci 2000; Nemes and Simmonds 1992) of sandwich structures with synthetic FRP faces. Dawood et al. (2009) tested 1200 mm by 1200 mm sandwich panels with GFRP faces and 25 mm and 50 mm thick foam cores with 3-D insertions under quasi-static bending. They developed a finite element model and used it to perform a parametric study to examine the effect of different parameters, including, panel thickness, face thickness and aspect ratio. Anderson and Madenci (2000) tested 76 mm by 76 mm sandwich panels with CFRP faces and 12.7 mm thick foam and honeycomb cores. They tested the panels using a drop weight impact test and found that panels subjected to low velocity impacts with little or no visible damage have the potential for significant internal damage. Schubel et al. (2004) tested 279 mm by 279 mm by 28 mm sandwich plates with 1.37 mm thick CFRP faces and a 25.4 mm thick PVC foam core under low velocity impacts. They found that general impact behaviour of the panels could be predicted by quasi-static testing. However, the indentation was more pronounced in plates tested under quasi-static loading. Betts et al. (2023) tested three large scale (1200 x 1200 mm) sandwich panels with FFRP faces of various thicknesses (one, two or three layers of flax fabric) and 75 mm thick foam cores under a concentrated quasi-static load inducing a two-way bending. The panels' ultimate strength and stiffness increased with thicker faces. Notably, localized deformations were observed in the top face and core within the loading zone, impacting the panels with thicker faces to a greater extent than the single-layer FFRP-faced panel. Another study by Selver et al. (2023) have shown

that natural and hybrid fiber composites absorbed more energy than that of glass fiber composites between 20 and 40J along with less fibre damages.

Currently, there is a gap in the field of research concerning the impact behaviour of two-way natural fiber (e.g. flax) FRP-foam sandwich panels. This is especially true for large-scale panels and large mass impacts representative of the structural engineering application scale (e.g. building cladding systems subjected to wind-borne debris). The aim of this study is to fill this gap by investigating the impact behaviour of large-scale (1220 mm by 1220 mm by 80 mm) sandwich panels with FFRP faces and 96 kg/m^3 polyisocyanurate foam cores.

EXPERIMENTAL PROGRAM

In this section, the experimental test matrix will be presented, the constituent material behaviour will be discussed, and the static and impact test set-ups will be presented.

Test Matrix

Nine large scale sandwich panels were fabricated and tested under impact loading applied at the center. Sandwich panels were comprised of FFRP faces and polyisocyanurate foam cores with a density of 96 kg/m^3. Each panel was 1220 mm by 1220 mm with a 75 mm thick foam core. Three face thicknesses of 1.15 mm, 2.30 mm, and 3.45 mm, corresponding to one, two, and three layers of flax fabric per face, were used, resulting in core-to-face thickness ratios of 65.1, 32.6, and 21.7, respectively. These dimensions were selected to simulate a potential real-world panel articulation as 1220 mm is a common dimension for building cladding materials. The main test parameters were the effect of face thickness and the effect of impact energy. The face

thicknesses were chosen to capture the two failure modes observed during the quasi-static flexural tests performed by Betts et al. (2023): face tensile rupture and core shear. The impact energies were chosen based on an equivalent failure energy, specifically 50%, 70% or 95% of the static failure energy (SFE), which is the area under the curve of load-deflection of identical specimens tested under concentrated quasi-static loading by Betts et al. (2023). To determine the equivalent failure energies, the first panel was tested at 95% SFE and it was found that this caused significant damage early in the testing. Therefore, the next panel was tested at 50% SFE and was not damaged throughout the testing. As such, the last specimen was tested at 70% SFE. The naming convention used in this study is as follows: XFL-DY, where X is the number of flax layers per face, FL stands for "Flax Layers", D stands for "Dynamic" and Y is the impact energy in N-m. As an example, a panel with three layers per face tested under an impact load of 656 N-m would be named 3FL-D656. The test matrix is presented in Table 1.

Materials

Balanced bidirectional 2x2 twill flax fabrics were used to fabricate the FFRP faces. The balanced bidirectional fabrics were used as they are commercially available and provide a simplified and easily repeatable manufacturing procedure. The flax fabric had a reported areal mass of 400 g/m^2 which was measured to be 410 g/m^2. The epoxy was a bio-based epoxy with an approximate bio-content of 25%, which was, at the time, the highest bio-content amongst commercially available epoxies. The properties of the epoxy were determined using ASTM D638 (ASTM 2014) in a previous study by Betts et al. (2018) which showed that the epoxy had a mean (± standard deviation) tensile

strength, initial elastic modulus and ultimate strain of 57.9 ± 0.4 MPa, 3.20 ± 0.13 GPa and 0.0287 ± 0.0018 mm/mm, respectively.

The tensile and shear properties of the FFRPs were determined using ASTM D3039 (ASTM 2017) and ASTM D3518 (ASTM 2018a), respectively, in a previous study by Betts et al. (2023). The tensile strength, initial elastic modulus and ultimate strain were found to be 70.0 ± 3.4 MPa, 6.35 ± 0.71 GPa and 0.0202 ± 0.0022 mm/mm, respectively, in the warp direction, and 51.3 ± 1.4 MPa, 5.64 ± 0.90 GPa and 0.0204 ± 0.0024 mm/mm, respectively, in the weft direction (Betts et al. 2023). Based on the same study, the shear strength, shear modulus and ultimate shear strain were found to be 23.1 ± 0.4 MPa, 1.26 ± 0.02 GPa, and 0.0562 ± 0.0053 mm/mm, respectively. Betts et al. (2023) also tested the 96 kg/m^3 polyisocyanurate (PIR) foam core material in shear (parallel to rise) using ASTM C273 (ASTM 2018b) and found that the shear strength, shear modulus and ultimate shear strain were 0.476 ± 0.102 MPa, 12.5 ± 0.8 MPa and 0.59 ± 0.018 mm/mm, respectively.

Specimen Fabrication

The specimen fabrication procedure for each panel is presented in Figure 1. The sections were cut down from the supplied size of 2440 mm x 1220 mm into 1220 mm square sections using a circular saw. The surface of the foam was cleaned of all dust and debris using a brush. The bio-based epoxy was applied to the surface of the foam as shown in Figure 1a. Then, a layer of the bidirectional flax fabric was placed on the wetted foam surface as shown in Figure 1b. The direction of the warp and weft was recorded on the side surface of the foam. Each subsequent layer (if required) of flax

fabric was placed such that the warp direction matched the previous layers. Specimens were fabricated with one, two or three layers of flax fabric per face. After the placement of each layer, a layer of bio-based epoxy was applied the surface of the flax fabric, as shown in Figure 1c. After the last layer was completed, a layer of parchment paper was placed on the top, as shown in Figure 1d. Then, an aluminum roller or a plastic scraper was used to remove any excess resin or entrapped air. A weighted flat board was placed on top of the panels and they cured under the weighted board for a minimum of 24 hours. Then, the opposite face was completed in the same manner.

Test Set-up and Instrumentation

Figure 2 shows the impact test set-up. The specimens were supported on a steel frame with a simulated pin connection at each side. The support frame was secured to a concrete strong floor. To stop the specimen from rebounding after an impact, a top frame of steel rods secured the sandwich specimens to the bottom steel frame using a u-bolt in each corner.

The specimens were impacted at the center by a 200 mm long, 140 mm diameter cylindrical impactor with a flat face. A diameter of 140 mm was selected to closely match the static tests performed by Betts et al. (2023). The impactor mass varied between a minimum mass of 10.5 kg to a maximum mass of 20 kg. To achieve the desired impact energy, maximizing the drop height was prioritized. However, for the testing of the 1FL specimens and specimen 2FL-D306, the minimum possible impactor weight limited the drop height. The impactor was dropped through a 150 mm diameter plastic guide pipe and the maximum drop height possible was 3250 mm. The bottom of the plastic guide

pipe was set approximately 100 mm above the top face of the specimens, to ensure that the impactor did not fully leave the guide pipe during the tests. To protect the strain gauge wires, a thin (approximately 3 mm thick) neoprene rubber mat was loosely placed on the specimen at the impact location. For consistency, this rubber mat was included in all tests, including the instrumented tests.

The test instrumentation is presented in Figure 3. The center deflection was recorded using a fast-action string potentiometer. The strains in both the warp and weft direction were measured using 350-ohm strain gauges with a 6 mm gauge length. All impact test data was recorded at a sample rate of 25,000 samples per second.

Panels were impacted multiple times under a drop weight. For the first impact, strain and displacement data were recorded for analysis. The subsequent impacts were (for the most part) performed without data acquisition to determine the number of impacts that a specimen could withstand before failure. All data presented in this study was processed using Python.

RESULTS AND DISCUSSIONS

First Impact

Each specimen was impacted multiple times with a drop weight at a fixed energy level: 50% static failure energy (SFE), 70% SFE or 95% SFE. The strain data of an impact at 95% SFE is presented in Figure 4. As shown in the figure, the bottom tensile strains behaved similarly for each specimen with comparable peak strains. However, the strains in the top faces were significantly different between the 1FL specimen and the 2FL and 3FL specimens. The top face strains in 1FL-D227 specimen showed the

highest values, while the top faces strains of specimens 2FL-D581 and 3FL-D656 show almost 50% lower strains under the same loading ratio. This observation is consistent with the results of the quasi-static tests presented by Betts et al. (2023) and shows there was likely significant energy absorbed by local indentation of the core and top face for the 2FL and 3FL panels. It should be noted that the first peak of the top face strain of 3FL-D656 in the warp direction shows tensile value, which could potentially be attributed to the local indentation of the core and top face.

In order to see the effect of the energy level on the impulse response of the sandwich panels, Figure 5 presents the impulse deflection and bottom warp strain responses of each impact test. The bottom warp strain was presented in addition to the displacement data because the displacement data was not obtained for some specimens due to failure of the string potentiometer connection point under the impact load. The bottom warp strain data was therefore presented to show the impulse response of the specimen in a location that was not significantly affected by the local deformation behaviour of the top face. Based on the results presented in Figure 5, the length of time for most of the impulses was unaffected by energy level. However, specimens impacted with the highest-level energies (2FL-D581, 3FL-D483 and 3FL-D656) presented a longer impulse duration. This prolonged impulse duration is attributed to the fact that these three specimens were the only specimens to exhibit signs of damage after the first impact as shown in Figure 6.

As shown in Figure 5, the impact energy did not have a significant effect on the maximum center displacement for most panels. The exception to this is specimen, 3FL-

D483, which was the only specimen that showed signs of damage for which displacement data was obtained. For each face thickness (i.e., 1FL, 2FL and 3FL), the specimens impacted at 95% SFE showed a significant increase of strain in the bottom face when compared with the 70% SFE test. It should be noted that for the 2FL and 3FL specimens, this is also paired with damage and a prolonged impulse duration as discussed above. However, based on the observations of 3FL-D483 and 3FL-D656, which both showed signs of damage, it is evident that this increase in strain was not necessarily caused by the damage. Therefore, it seems that there is a threshold between 70% and 95% where the strain developed in the bottom face increases dramatically.

Upon further examination of Figure 5, it is evident that the shape of the bottom warp strain impulse response is affected by the panel face thickness, but not affected by the impact energy. Generally, the shape of the impulse was approximately in the shape of a half sine-wave. However, as the panel face thickness decreased, the presence of a higher frequency response becomes evident. The higher frequency response is likely suppressed in the thicker faced specimens due to the local deformation developed in these panels. It should be noted that this behaviour is also present in the 1FL specimens' displacement responses, however it is not as prominent as in the strain responses.

Prior to testing specimens 2FL-D306 and 3FL-D345, each was tested once at 119 J to directly compare their impulse response with 1FL-D119. Similarly, 2FL-D428 and 3FL-D483 were each tested once at 167 J to directly compare their impulse response with 1FL-D167. It was assumed that these specimens could be tested once at these low

energy levels (< 30% SFE) and still be considered intact for their respective tests. This assumption was based on the fact that the points corresponding to 30% SFE on the stress-strain plots of the statically tested panels by Betts et al. (2023) are well within the linear portion of the curves which indicates that no damage had yet occurred at this energy.

Figure 7 presents the effect of face thickness on the impulse response of the sandwich panels. As expected, for each energy level, 119 J and 167 J, the center displacement increased with a decrease in face thickness. Additionally, the impulse duration increased with a decrease in face thickness. This indicates that specimens with a more global loading response (i.e., plate deflection) have a longer impulse duration than specimens with a more local loading response (i.e., indentation of core and top face). In future studies, it would be beneficial to measure the indentation of the top face during an impact event. However, this would present considerable challenges with the test set-up.

Effect of Multiple Impact Events

To understand the panels' resiliency, each specimen was impacted multiple times targeting a total number of 100 impacts or until obvious ultimate failure. The number of impacts before obvious ultimate failure for each specimen is presented in Table 2. It should be noted that determining the ultimate failure visibly in the two-way panels was not accurate, and the additional tests were performed to gain understanding of the behaviour during damage development. One observation made by performing these additional impacts was that panels susceptible to core shear failure under quasi-static

testing were less resilient than panels susceptible to tensile failure of the bottom face. For the 95% SFE specimens, 1FL-D227, 2FL-D581 and 3FL-D656, only the 1FL-D227 specimen remained relatively undamaged after multiple impact events. This shows that the FFRP faces are likely more resilient than the foam cores. Therefore, FFRP-foam sandwich structures that will be subjected to impact loads should be designed such that ultimate failure is controlled by the FFRP faces, if possible.

For two specimens, 3FL-D345 and 3FL-D483, the strain data was recorded for each impact event to show the damage progression due to multiple impacts. Note that panel 3FL-D345 did not experience perceived ultimate failure during the impact tests and was impacted 100 times whereas panel 3FL-D483 was impacted only 8 times due to perceived ultimate failure by delamination of the top face under the impact area. The bottom weft strain impulse responses for each specimen after multiple impacts are presented in Figure 8.

For panel 3FL-D345, the impulse response was not affected by multiple impacts. However, panel 3FL-D483 was significantly affected by the number of impacts and shows a clear damage progression as the number of impacts increased. As previously mentioned, panel 3FL-D483 showed visible damage after the first impact event and it also showed a prolonged impulse duration (Figure 5). As shown in Figure 8, the impulse duration increased further, and the strain response became softer after each subsequent impact. The visible progression of the damage is presented in Figure 9. There was an obvious visible damage progression, but the delamination was not observed until the eighth impact, at which point the tests were stopped. However, upon examination of the

impulse response plots shown in Figure 8, the progression of internal damage was more substantial than the damaged observed during testing.

FINITE ELEMENT MODELLLING

Betts et al. (2023) modelled similar panels under quasi-static loads. In this study, new finite element (FE) models were created using the commercial program LS DYNA to perform the impact analyses of the sandwich panels. A photo of the impact FE model is presented in Figure 10. A comparison of the quasi-static and impact FE models is presented in Table 3. It should be noted that as the models examined only low velocity impacts, it is assumed that the strain rate would have little effect on the results. Additionally, the FE models were used to examine the responses under only one impact and damage accumulation was not considered. Therefore, the effect of strain rate was not considered in the modelling.

In both the quasi-static (Betts et al. 2023) and impact models, the element formulation -2 per Dynamore (2018) was used. This is an accurate formulation for elements with poor aspect ratios. It is suggested that this be used for implicit analyses, which is why it was chosen for the quasi-static analysis. However, as shown in Table 3, the impact analysis was completed using the explicit solver with a time step of $5x10^{-5}$ seconds. The same element formulation was used for consistency between the models.

The same material models were used in the impact model, except for the steel impactor, which was changed from the RIGID material model in the quasi-static modelling to the ELASTIC material model for the impact modelling. This is because the boundary condition did not require a rigid part as in the quasi-static model. Also note

that for the models presented in this study, a constant material density was used for the impactor and an initial velocity was applied such that the required impact energy was obtained.

As in the study by Betts et al. (2023), the face materials were modelled using the NONLINEAR_ORTHOTROPIC (MAT_040) using the average stress-strain test data in both the warp and weft directions. It is important to note that this material model does not allow for different material properties in tension and compression. Therefore, understanding that during the impact impulse the bottom face is generally in tension and the top face is generally in compression, the material models were implemented as such. This procedure was also used by Betts et al. (2023).

The core was modelled using material model MAT_057, LOW_DENSITY_FOAM. This model takes the compressive stress-strain curve of the foam as an input. The stress-strain curve for the 96 kg/m^3 PIR foam presented by Codyre et al. (2018) was used for the modelling.

The support conditions were changed to match the experimental tests. To do this, supports were added to the top face of the panel as shown in Figure 11. These top supports were modelled to simulate the specimen rebound restraint present in the experiments.

Mortar contacts were used in the quasi-static model as it was suggested by the implicit guidelines by Dynamore (2018). However, it was determined that for explicit analyses, the mortar contacts caused significant penetration and that the non-mortar variation of the same contact types was more accurate. The contact parameters were

kept the same for consistency. That is why the static and dynamic coefficient of friction was set to 0.0001 between the panel and the supports and to 0.8 between the impactor, rubber pad and the top face of the panel.

A mesh convergence study was completed for the quasi-static models in the study by Betts et al. (2023). It was determined that the Moderate-R mesh offered adequate accuracy while maintaining a reasonable computation runtime. Therefore, for consistency, the Moderate-R mesh was also used for the impact modelling.

Model Verification

The FE models developed in this study were verified using the test data. Figure 12 shows a comparison of the face strains between the FE models and the respective experimental tests at impact levels of 50%, 70% and 95% SFE. As shown in the figure, the models were able to capture the impulse duration and the maximum strains induced in the top and bottom faces.

The models were also verified using the displacement data for the specimens tested under constant energy levels 119 J and 167 J which are the equivalents of the 50% and 70% SFE for the 1FL panel. The verification of the models impacted at 119 J and 167 J are presented in Figure 13 and Figure 14, respectively. These figures show that for low level impacts, the model was able to capture both the center displacement and face strain behaviour of the panels. It should be noted that for some parts of the experimental curves, especially in terms of strains, the agreement with the numerical results is not precise. Considering the complexity of the problem, the performance of the FE models is satisfactory. In contrast, the model and results of counterpart panels

tested under quasi-static loading are available in Betts et al. (2023). The models were then used to perform a parametric study to examine the effect of core density and core thickness.

Parametric Study

A parametric study was completed to see the effect of core density, core thickness, and face thickness. Core densities of 32 kg/m^3, 64 kg/m^3 and 96 kg/m^3 and core thicknesses of 25.4 mm, 50.8 mm and 76.2 mm were analysed. For this study, an impact energy of 80 J was selected to directly compare all the models. This energy level was selected as it is below the anticipated failure energy of all panel types and this assumption was verified through examination of the results of each model.

Effect of Core Density

To examine the effect of core density, panels with three core densities were modelled: 32 kg/m^3, 64 kg/m^3 and 96 kg/m^3 (C32, C64 and C96). The effect of core density on the center displacement caused by an impact of 80 J is presented in Figure 15. Based on the figure, the impulse duration increased with a decrease in core density for panels with all face thicknesses. Considering the impulse duration to be from the start of the downward displacement the panel returns to the original position, the impulses of the 3FL panels were approximately 5.6 ms, 7.5 ms, and 10.6 ms for C96, C64 and C32 panels, respectively. That is an increase of 34% between C96 and C64 panels and an increase of 89% between the C96 and the C32 panels. However, the general shape of the impulses remained the same. Additionally, the maximum center displacement also

increased with a decrease in core density and the largest increases were between the C64 and C32 panels.

Effect of Face Thickness

The effect of the face thickness on the impulse behaviour can be seen in Figure 15 by comparing the plots of the same core densities in the sub-figures (a), (b) and (c). As expected, the maximum displacement decreased with the increase in face thickness. The face thickness did not have a significant effect on the impulse duration of the panels with C32 cores. However, upon examination, the impulse duration was affected by face thickness for panels with higher density cores (C64 and C96). For instance, the impulse durations of the C64 panels were approximately 6.9 ms, 7.5 ms, and 8.1 ms for the 3FL, 2FL and 1FL panels, respectively. A similar trend is also seen in the C96 panels.

It is likely that the impulse duration of the C32 panels was not affected by face thickness due to a higher amount of shear deformation. A visual comparison of the maximum downward displacement shape of panels, 3FL-C32, 3FL-C64 and 3FL-C96 is presented in Figure 16. The comparison shows that the C32 panel undergoes significantly more shear deformation than the C64 and C96 panel as evidenced by the straight line between the support and the load area.

Effect of Core Thickness

To examine the effect of core thickness, panels with three core thicknesses were modelled: 25.2 mm, 50.8 mm and 76.2 mm (identified as CT25, CT50 and CT75, respectively). The effect of the core thickness on the impulse response of the sandwich panels is presented in Figure 17. The maximum displacements and impulse durations

increased with a decrease in core thickness for all panels, as expected. The largest increase in impulse duration due to one step decrease in core thickness was 77% between 1FL-C96-CT50 and 1FL-C96-CT25, increasing from approximately 8.75 ms to 15.63 ms, Additionally, for panels with thin cores (CT25), the face thickness had a significant effect on the maximum displacement and impulse duration. This is because the thinner panels experienced a more flexural type of deformation than the thicker core panels (50.8 mm and 76.2 mm). Therefore, as the faces resist the majority of the flexural stresses, the face thickness is an important parameter for panels with thin cores.

Future Studies

The intent of this research was to show the viability of sandwich structures with FFRP faces for use in infrastructure. The research has shown that these sandwich structures exhibit remarkable resilience and relatively high strengths. However, to incorporate these structures into new design codes and subsequently new infrastructure, more research is required including, but not limited to:

- Performing more tests to build the experimental database and to ensure that there is enough experimental data to develop design resistance factors and to perform reliability studies.
- Exploring the size effect on the behaviour of sandwich panels with FFRP faces, specifically looking at the effects of larger span lengths and different core thicknesses.

- Improving the FE modeling with advanced features such as smeared crack analysis and strain rate effects.
- Investigating the effect of fire, wet/dry, freeze/thaw conditions on sandwich panels with FFRP faces.

CONCLUSIONS

Based on the experimental and numerical investigations, the following conclusions were drawn:

- The impact energy level did not have a significant effect on the center displacement or impulse duration of the panels. However, when damage was observed, both the center displacement and the impulse duration increased significantly.
- The impact specimens were tested multiple times under set impact energies up to 100 times or until failure was observed. Failure was difficult to determine as it was often initiated by the core material and was not visible. For specimens without damage, the impulse shape and duration was not affected after each impact, however for damaged panels, the impulse duration increased, and the impulse shape changed.
- The parametric study showed that, generally, impulse duration and maximum deflection both increased with a decrease in face thickness, core thickness and core density. For sandwich panels with three face layers, the impulse duration was increased by 89% when the core density was decreased from 96 kg/m^3 to 32 kg/m^3. For sandwich panels with core densities of 64 kg/m^3, the impulse duration increased by 17% when the number of FFRP layers per face was decreased from three to one.

ACKNOWLEDGEMENTS

The authors would like to thank Anurag Mishra, Lucas Marques, Jordan Maerz and Jesse Keane for their assistance in the lab. The authors would also like to acknowledge and thank NSERC, Queen's University, and Dalhousie University for their financial support.

DATA AVAILABILITY STATEMENT

Data associated with this study is available upon request.

REFERENCES

Abrate, S. (1997). Localized impact on sandwich structures with laminated facings. 50:69. https://doi.org/10.1115/1.3101689.

Akil Hazizan M, Cantwell WJ. (2002). The low velocity impact response of foam-based sandwich structures. Compos Part B Eng; 33:193–204. https://doi.org/10.1016/S1359-8368(02)00009-4.

Anderson T, Madenci E. (2000). Experimental investigation of low-velocity impact characteristics of sandwich composites. Compos Struct; 50:239–47. https://doi.org/10.1016/S0263-8223(00)00098-2.

ASTM. (2014). Standard test method for tensile properties of plastics. Annual Book of ASTM Standards. ASTM D638. West Conshohocken, PA: ASTM.

ASTM. (2017). Standard test method for tensile properties of polymer matrix composite materials. Annual Book of ASTM Standards. ASTM D3039/D3039M. West Conshohocken, PA: ASTM.

ASTM. (2018a). Standard test method for in-plane shear response of polymer matrix composite materials by tensile test of a ±45° laminate. Annual Book of ASTM Standards. ASTM D3518/D3518M. West Conshohocken, PA: ASTM.

ASTM. (2018b). Standard test method for shear properties of sandwich core materials. Annual Book of ASTM Standards. ASTM C273/C273M. West Conshohocken, PA: ASTM.

Baley C, Le Duigou A, Bourmaud A, Davies P. (2012). Influence of drying on the mechanical behaviour of flax fibres and their unidirectional composites. Compos Part A Appl Sci Manuf; 43:1226–33. https://doi.org/10.1016/j.compositesa.2012.03.005.

Bambach MR. (2017). Thin-Walled Structures Compression strength of natural fi bre composite plates and sections of flax , jute and hemp. Thin Walled Struct; 119:103–13. https://doi.org/10.1016/j.tws.2017.05.034.

Bensadoun F, Vallons KAM, Lessard LB, Verpoest I, Van Vuure AW. (2016). Fatigue behaviour assessment of flax-epoxy composites. Compos Part A Appl Sci Manuf; 82:253–66. https://doi.org/10.1016/j.compositesa.2015.11.003.

Besant T, Davies GAO, Hitchings D. (2001). Finite element modelling of low velocity impact of composite sandwich panels. Compos - Part A Appl Sci Manuf; 32:1189–96. https://doi.org/10.1016/S1359-835X(01)00084-7.

Betts D, Sadeghian P, Fam A. (2018). Experimental Behavior and Design-Oriented Analysis of Sandwich Beams with Bio-Based Composite Facings and Foam Cores. J Compos Constr; 22:1–12.

Betts D, Sadeghian P, Fam A. (2020). Experiments and nonlinear analysis of the impact behaviour of sandwich panels constructed with flax fibre-reinforced polymer faces and foam cores. J Sandw Struct Mater. https://doi.org/10.1177/1099636220925073.

Betts D, Sadeghian P, Fam A. (2023). Finite Element Modelling and Experimental Verification of Two-Way Sandwich Panels Made of Natural Fiber Composites. Journal of Composites for Construction, 27(1),04022101. https://doi.org/10.1061/JCCOF2.CCENG-3897.

Betts D, Sadeghian P, Fam (2021). A. Post-Impact Residual Strength and Resilience of Sandwich Panels with Natural Fiber Composite Faces. J Build Eng; 38:102184.

Betts D, Sadeghian P, Fam A. (2020). Structural Behavior of Sandwich Beams with Flax Fiber-Reinforced Polymer Faces and Cardboard Cores under Monotonic and Impact Loads. J Archit Eng; 26:1–12. https://doi.org/10.1061/(ASCE)AE.1943-5568.0000409.

Christian SJ, Billington SL. (2011). Mechanical response of PHB- and cellulose acetate natural fiber-reinforced composites for construction applications. Compos Part B; 42:1920–8. https://doi.org/10.1016/j.compositesb.2011.05.039.

Cicala G, Cristaldi G, Recca G, Latteri A. (2010). Composites Based on Natural Fibre Fabrics. In: Dubrovski PD, editor. Woven Fabr. Eng., IntechOpen; https://doi.org/10.5772/10465.

CoDyre L, Mak K, Fam A. (2018). Flexural and axial behaviour of sandwich panels with bio-based flax fibre-reinforced polymer skins and various foam core

densities. J Sandw Struct Mater; 20:595–616. https://doi.org/10.1177/1099636216667658.

Dai J, Hahn HT. (2003). Flexural behavior of sandwich beams fabricated by vacuum-assisted resin transfer molding. Compos Struct; 61:247–53. https://doi.org/10.1016/S0263-8223(03)00040-0.

Daniel IM, Abot JL, Schubel PM, Luo JJ. (2012). Response and Damage Tolerance of Composite Sandwich Structures under Low Velocity Impact. Exp Mech; 52:37–47. https://doi.org/10.1007/s11340-011-9479-y.

Dawood M, Taylor E, Rizkalla S. (2010). Two-way bending behavior of 3-D GFRP sandwich panels with through-thickness fiber insertions. Compos Struct; 92:950–63. https://doi.org/10.1016/j.compstruct.2009.09.040.

Dynamore. (2018). Guideline for implicit analyses using LS-DYNA:1–87.

Fam A, Sharaf T. (2010). Flexural performance of sandwich panels comprising polyurethane core and GFRP skins and ribs of various configurations. Compos Struct; 92:2927–35. https://doi.org/10.1016/j.compstruct.2010.05.004.

Fu Y, Sadeghian P. (2020). Flexural and shear characteristics of bio-based sandwich beams made of hollow and foam-filled paper honeycomb cores and flax fiber composite skins. Thin-Walled Struct; 153:106834. https://doi.org/10.1016/j.tws.2020.106834.

Gupta N, Woldesenbet E, Kishore, Sankaran S. (2002). Response of Syntactic Foam Core Sandwich Structured Composites to Three-Point Bending. J Sandw Struct Mater; 4:249–72. https://doi.org/10.1106/109963602024140.

Hristozov D, Wroblewski L, Sadeghian P. (2016). Long-term tensile properties of natural fibre-reinforced polymer composites: Comparison of flax and glass fibres. Compos Part B Eng; 95:82–95. https://doi.org/10.1016/j.compositesb.2016.03.079.

Huo R, Liu W, Wan L, Fang Y, Wang L. (2015). Experimental Study on Sandwich Bridge Decks with GFRP Face Sheets and a Foam-Web Core Loaded under Two-Way Bending. Adv Mater Sci Eng. https://doi.org/10.1155/2015/434721.

Mak K, Fam A, Macdougall C. (2015). Flexural Behavior of Sandwich Panels with Bio-FRP Skins Made of Flax Fibers and Epoxidized Pine-Oil Resin. J Compos Constr; 19:1–13. https://doi.org/10.1061/(ASCE)CC.1943-5614.0000560.

Mak K, Fam A. (2019). Freeze-thaw cycling effect on tensile properties of unidirectional flax fiber reinforced polymers. Compos Part B Eng; 174:106960. https://doi.org/10.1016/j.compositesb.2019.106960.

Manalo A, Surendar S, van Erp G, Benmokrane B. (2016). Flexural behavior of an FRP sandwich system with glass-fiber skins and a phenolic core at elevated in-service temperature. Compos Struct; 152:96–105. https://doi.org/10.1016/j.compstruct.2016.05.028.

Manalo AC, Aravinthan T, Karunasena W, Islam MM. (2010). Flexural behaviour of structural fibre composite sandwich beams in flatwise and edgewise positions. Compos Struct; 92:984–95. https://doi.org/10.1016/j.compstruct.2009.09.046.

McCracken A, Sadeghian P. (2018). Corrugated cardboard core sandwich beams with bio-based flax fiber composite skins. J Build Eng; 20:114–22. https://doi.org/10.1016/j.jobe.2018.07.009.

Nemes JA, Simmonds KE. (1992). Low-Velocity Impact Response of Foam-Core Sandwich Composites. J Compos Mater; 26:500–19. https://doi.org/10.1177/002199839202600403.

Petras A, Sutcliffe MPF. (1999). Failure mode maps for honeycomb sandwich panels. Compos Struct; 44:237–52. https://doi.org/10.1016/S0263-8223(98)00123-8.

Qi Y, Fang H, Liu W. (2016). Experimental study of the bending properties and deformation analysis of web-reinforced composite sandwich floor slabs with four simply supported edges. PLoS One; 11:1–26. https://doi.org/10.1371/journal.pone.0149103.

Ramesh M, Palanikumar K, Reddy KH. (2017). Plant fibre based bio-composites : Sustainable and renewable green materials. Renew Sustain Energy Rev; 79:558–84. https://doi.org/10.1016/j.rser.2017.05.094.

Sadeghian P, Hristozov D, Wroblewski L. (2018). Experimental and analytical behavior of sandwich composite beams: Comparison of natural and synthetic materials. J Sandw Struct Mater; 20:287–307. https://doi.org/10.1177/1099636216649891.

Satasivam S, Bai Y, Yang Y, Zhu L, Zhao XL. (2018). Mechanical performance of two-way modular FRP sandwich slabs. Compos Struct; 184:904–16. https://doi.org/10.1016/j.compstruct.2017.10.026.

Schubel PM, Luo J-J, Daniel IM. (2005). Low velocity impact behavior of composite sandwich panels. Compos Part A Appl Sci Manuf; 36:1389–96. https://doi.org/10.1016/j.compositesa.2004.11.014.

Selver E, Dalfi H, Yousaf Z. (2002). Investigation of the impact and post-impact behaviour of glass and glass/natural fibre hybrid composites made with various stacking sequences: Experimental and theoretical analysis. Journal of Industrial Textiles. 51(8):1264-94.

Sharaf T, Shawkat W, Fam A. (2010). Structural performance of sandwich wall panels with different foam core densities in one-way bending. J Compos Mater; 44:2249–63. https://doi.org/10.1177/0021998310369577.

Sparnins E. (2006). Mechanical properties of flax fibers and their composites. Lulea University of Technology.

Torre L, Kenny JM. (2000). Impact testing and simulation of composite sandwich structures for civil transportation. Compos Struct; 50:257–67. https://doi.org/10.1016/S0263-8223(00)00101-X.

Yan L, Kasal B, Huang L. (2016). A review of recent research on the use of cellulosic fibres, their fibre fabric reinforced cementitious, geo-polymer and polymer composites in civil engineering. Compos Part B Eng; 92:94–132. https://doi.org/10.1016/j.compositesb.2016.02.002.

Table 1. Test matrix for 1220 mm x 1220 mm sandwich panel tests

Specimen ID	Face Layers (Thickness, mm)	Core-to-Face Thickness Ratio	Impact Energy, N-m	Impact Energy, % Failure Energy	Number of Specimens	Number of Impacts
1FL-D119	1 (1.17)	65.1	119	50	1	20
1FL-D167	1 (1.17)	65.1	167	70	1	100
1FL-D227	1 (1.17)	65.1	227	95	1	100
2FL-D306 *	2 (2.34)	32.6	306	50	1	52
2FL-D428 †	2 (2.34)	32.6	428	70	1	12
2FL-D581	2 (2.34)	32.6	581	95	1	5
3FL-D345 *	3 (3.51)	21.7	345	50	1	100
3FL-D483 †	3 (3.51)	21.7	483	70	1	8
3FL-D656	3 (3.51)	21.7	656	95	1	15
Total	-	-	-	-	12	412

* *Tested once at an impact energy of 119 J before subsequent testing*

† *Tested once at an impact energy of 167 J before subsequent testing*

Table 2. Number of impacts to failure

Specimen ID	Impacts to Ultimate Failure	Notes
1FL-D119	20	Tests stopped. Probable delamination in top face
1FL-D167	DNF*	Visible tensile crack in matrix on bottom face
1FL-D227	DNF	Visible tensile cracks in matrix on bottom face
2FL-D306	52	Probable delamination in top face before 52 impacts
2FL-D428	11	Substantial cracking and fibre rupture in top face
2FL-D581	4	Assumed shear failure within and significant cracking of top face
3FL-D345	DNF	No visible signs of damage
3FL-D483	8	Assumed shear failure within and significant cracking of top face
3FL-D656	6	Assumed shear failure within and significant cracking of top face

*DNF: did not fail.

Table 3. Comparison of quasi-static and impact FE models

Item	Quasi-Static Models Betts et al (2023)	Impact Models Current Study
Solver	Implicit	Explicit
Element Types	All solids	All solids
Element Formulations	-2	-2
Face Material	NONLINEAR_ORTHOTROPIC	NONLINEAR_ORTHOTROPIC
Core Material	LOW_DENSITY_FOAM	LOW_DENSITY_FOAM
Supports Material	ELASTIC	ELASTIC
Impactor Material	RIGID	ELASTIC
Rubber Material	BLATZ-KO_RUBBER	BLATZ-KO_RUBBER
Face-Core Contacts	AUTOMATIC_SURFACE_TO _SURFACE_MORTAR_TIED	TIED_SURFACE_TO _SURFACE
Panel-Support Contacts	AUTOMATIC_SURFACE_TO _SURFACE_MORTAR_TIED	AUTOMATIC_SURFACE_TO _SURFACE
Support Locations	Bottom edges	Top and bottom edges
Load Application	PRESCRIBED_MOTION_ RIGID	INITIAL_VELOCITY_ GENERATION
Mesh Type	Moderate-R	Moderate-R
Failure	Compression wrinkling, face failure and core shear failure considered in post-processing	N/A

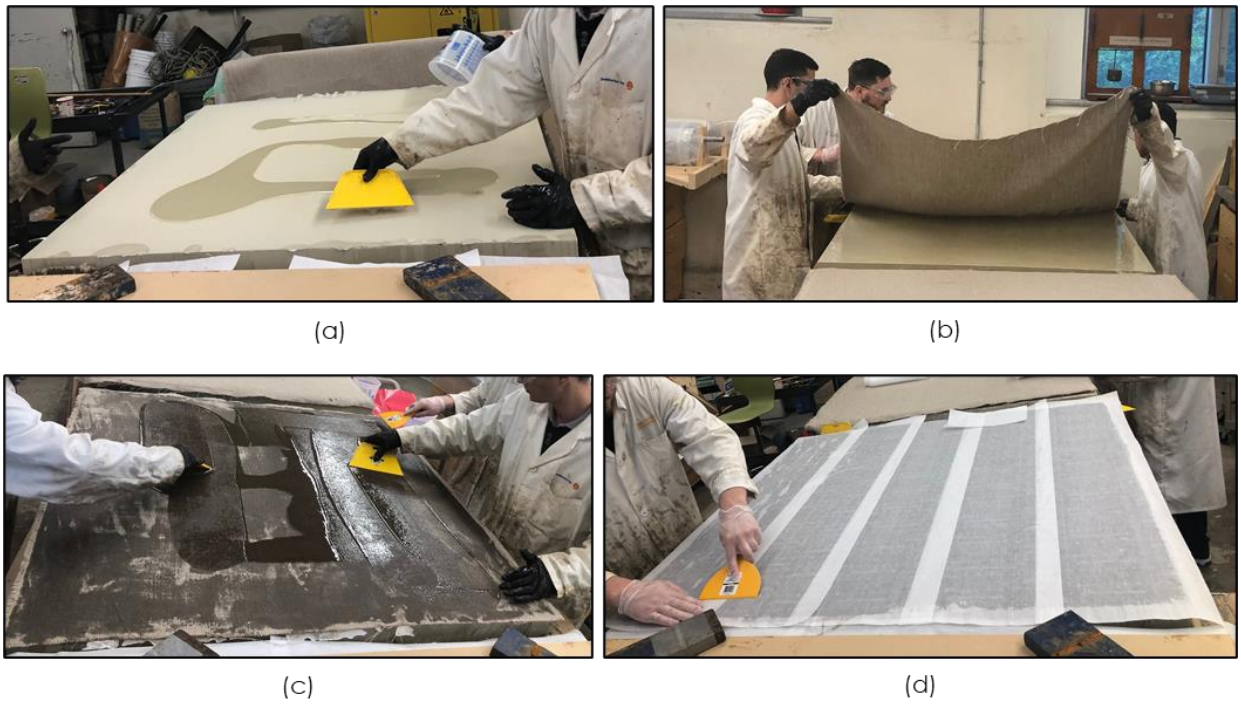

Figure 1. Specimen fabrication (a) applying bio-based epoxy on foam surface; (b) placement of flax fabric; (c) applying bio-based epoxy to flax fabric; and (d) placement of parchment paper

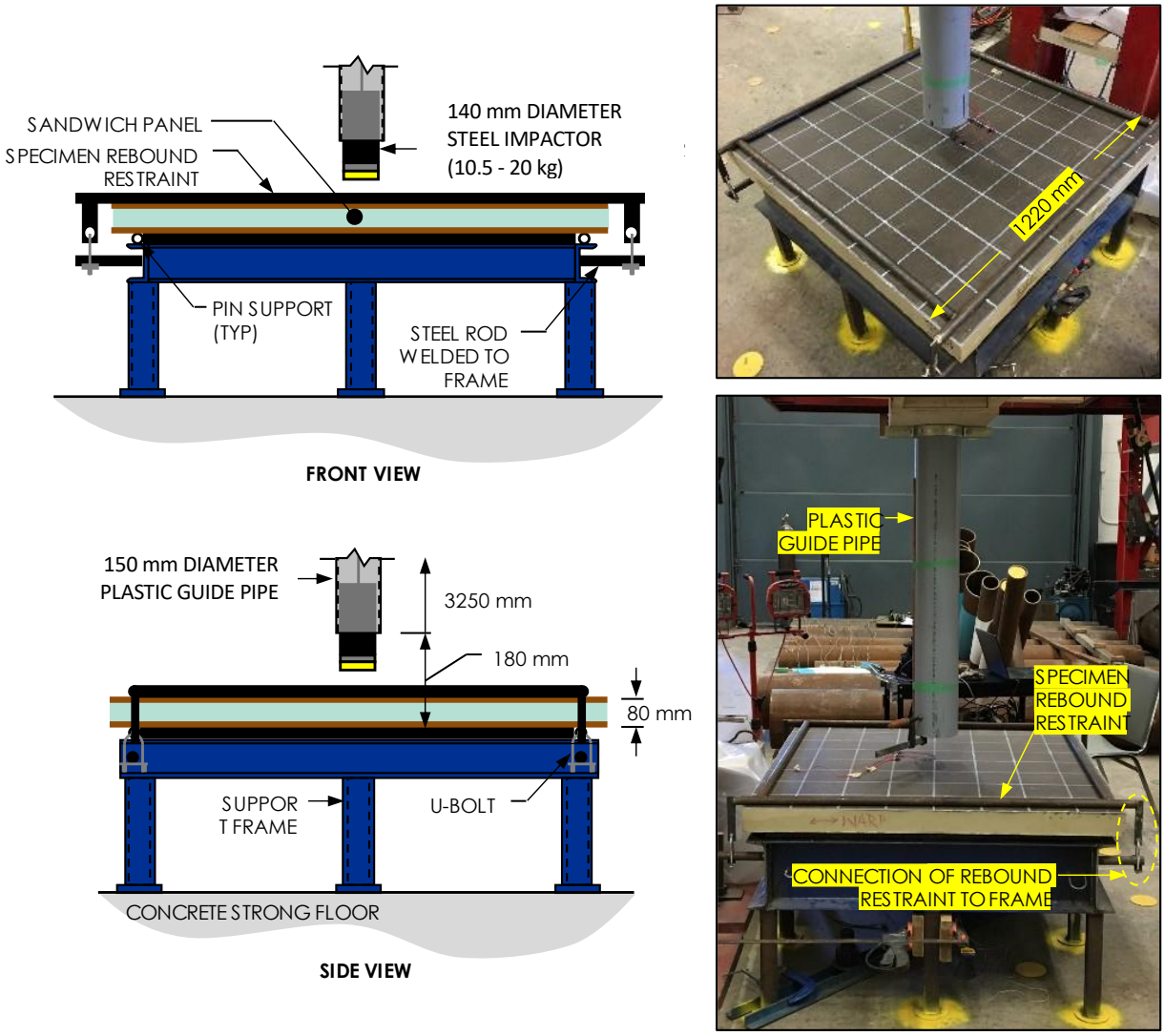

Figure 2. Impact test set-up

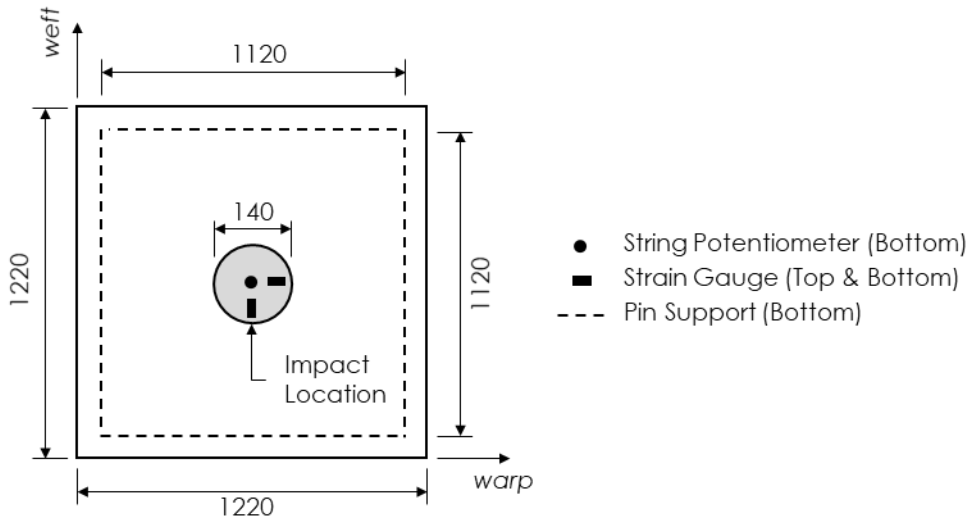

Figure 3. Test instrumentation (not to scale, dimensions are in mm)

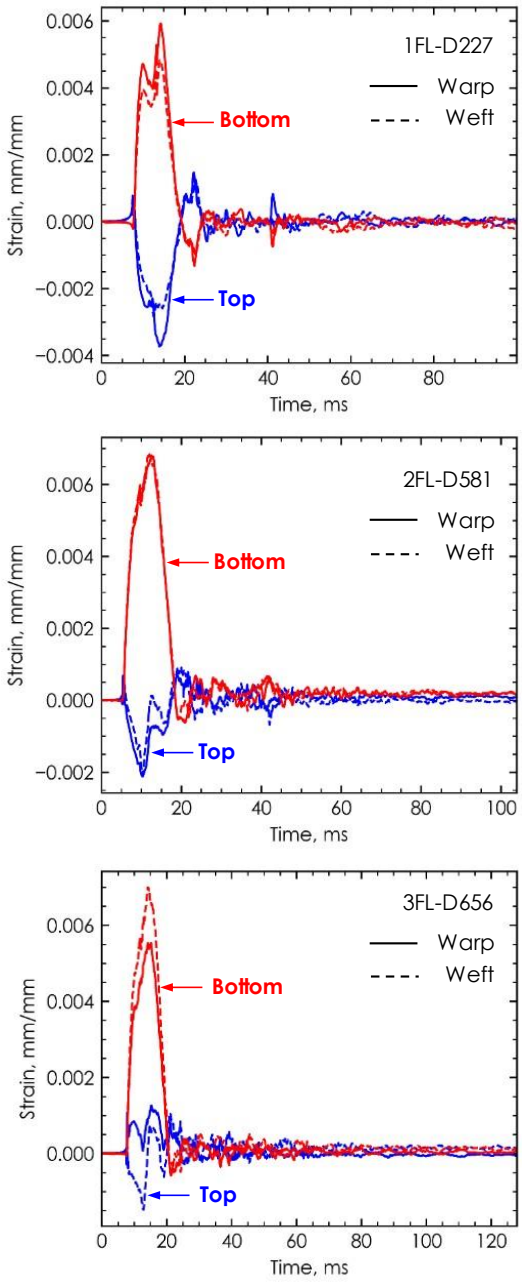

Figure 4. Strain data of 95% static failure energy impact on intact specimens

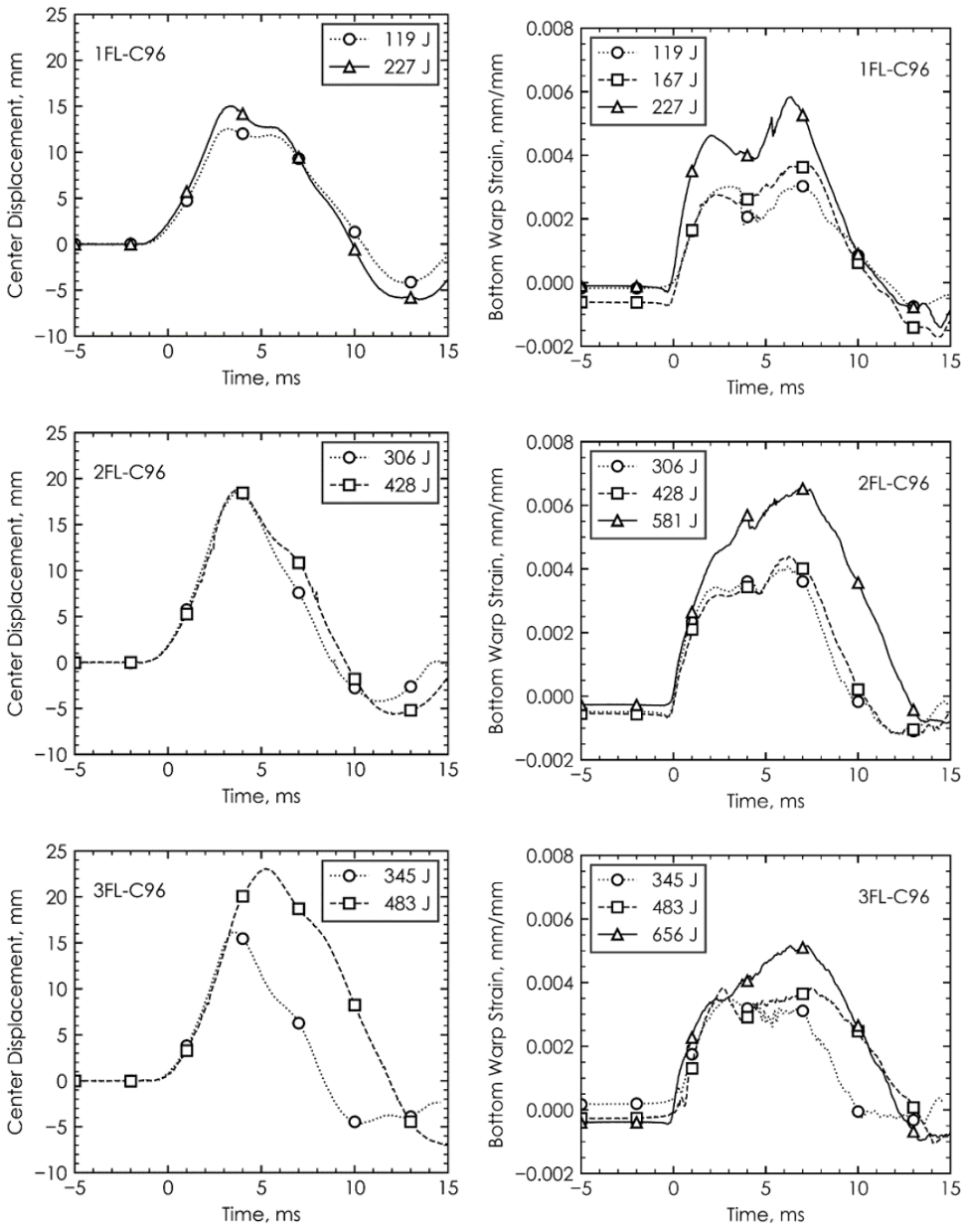

Figure 5. Deflection and bottom warp strain data for the impact on intact specimens

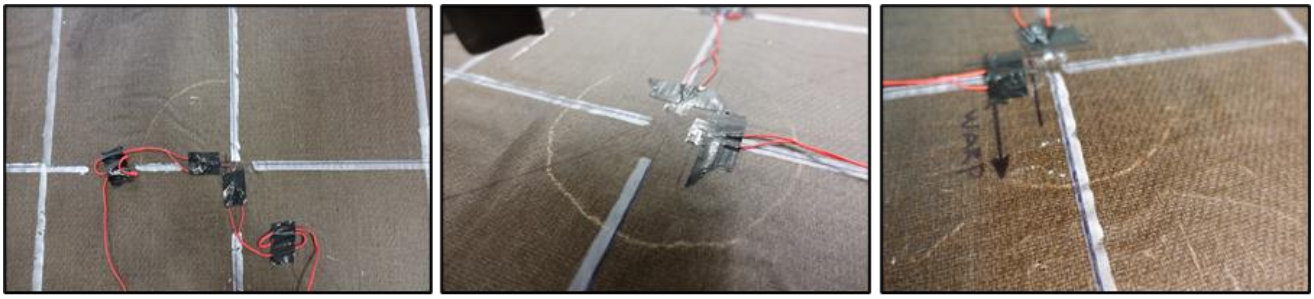

Figure 6. Visible damage after first impact

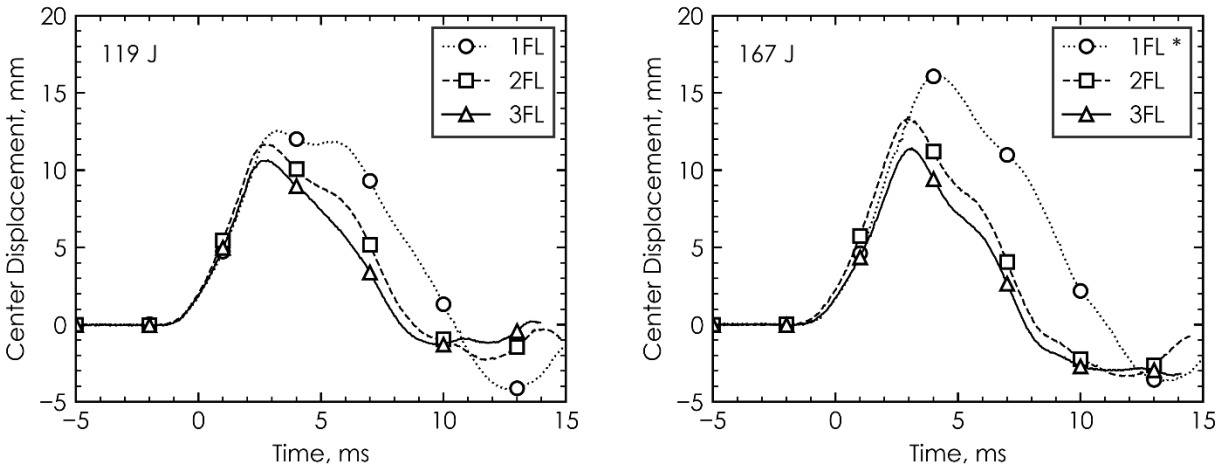

Figure 7. Effect of face thickness on displacement behaviour of a panel subjected to a set energy level (* deflection data for 1FL-D167 is presented for the second impact event as the deflection data was not captured during first impact event)

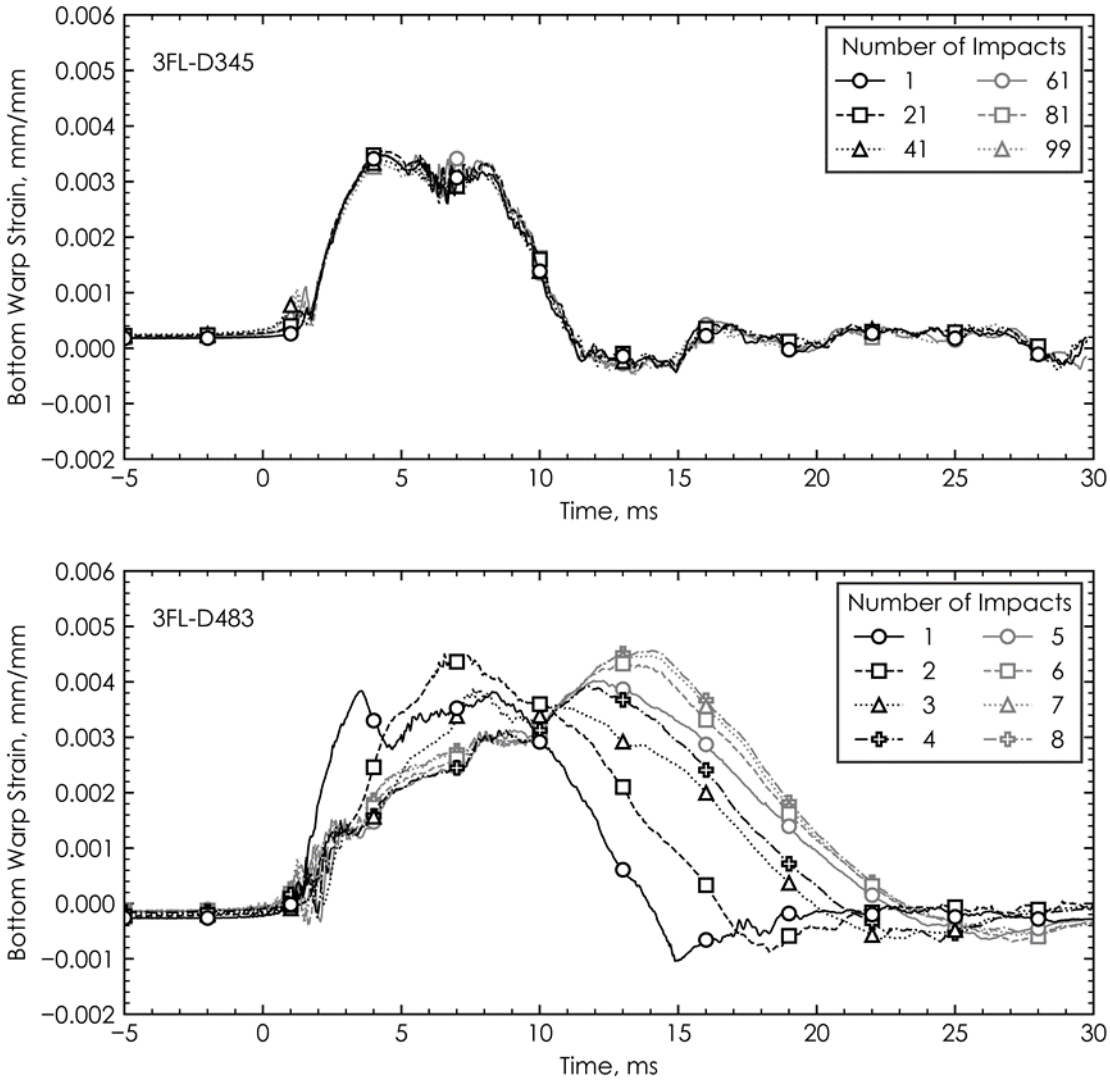

Figure 8. Impulse responses of 3FL-D345 and 3FL-D483 after multiple impact events

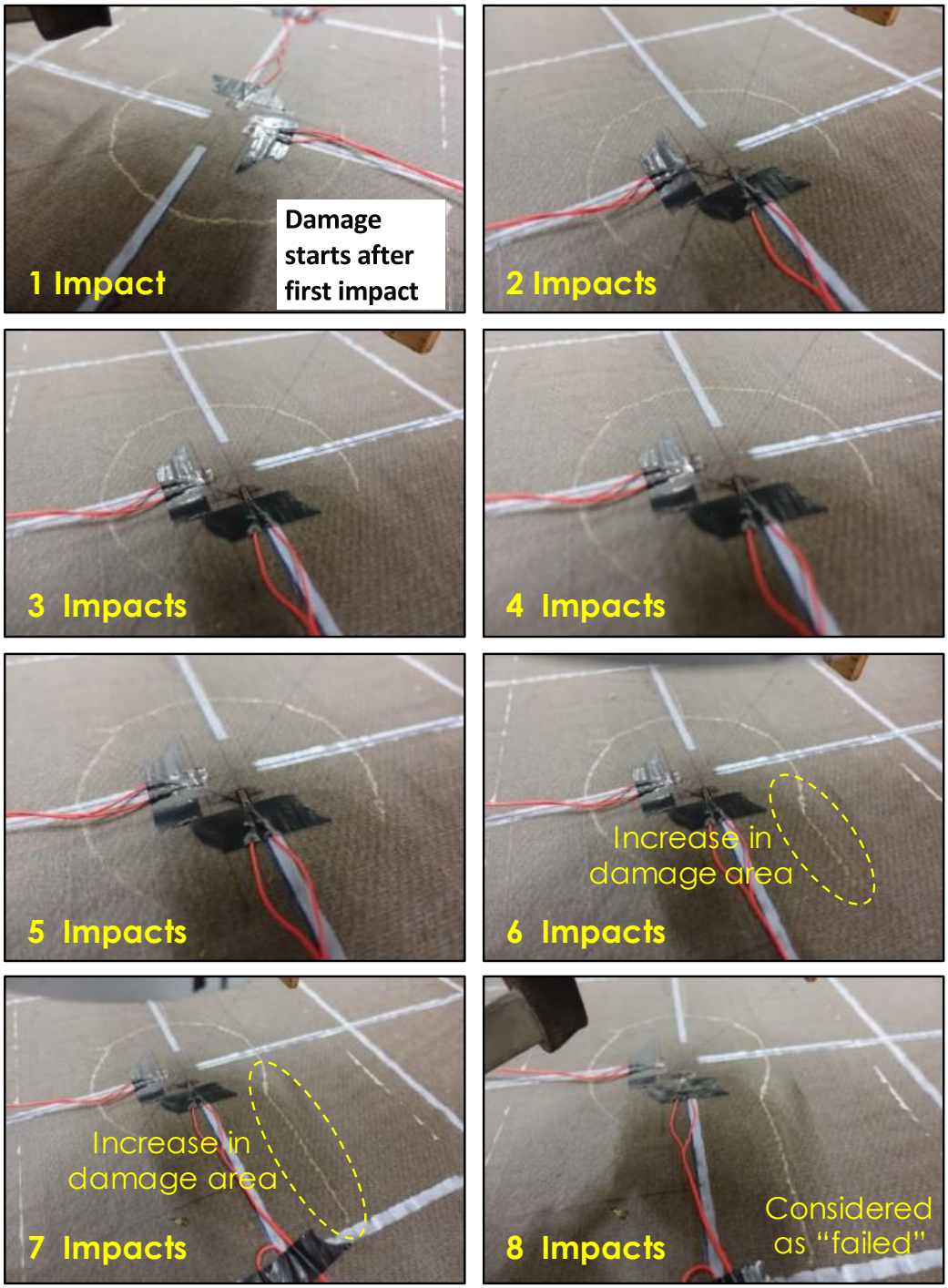

Figure 9. Observed damage progression of 3FL-D483 – significant damage observed after first impact, followed by slow increase of damage until, after six impacts, damage increases significantly and continues after next two impacts

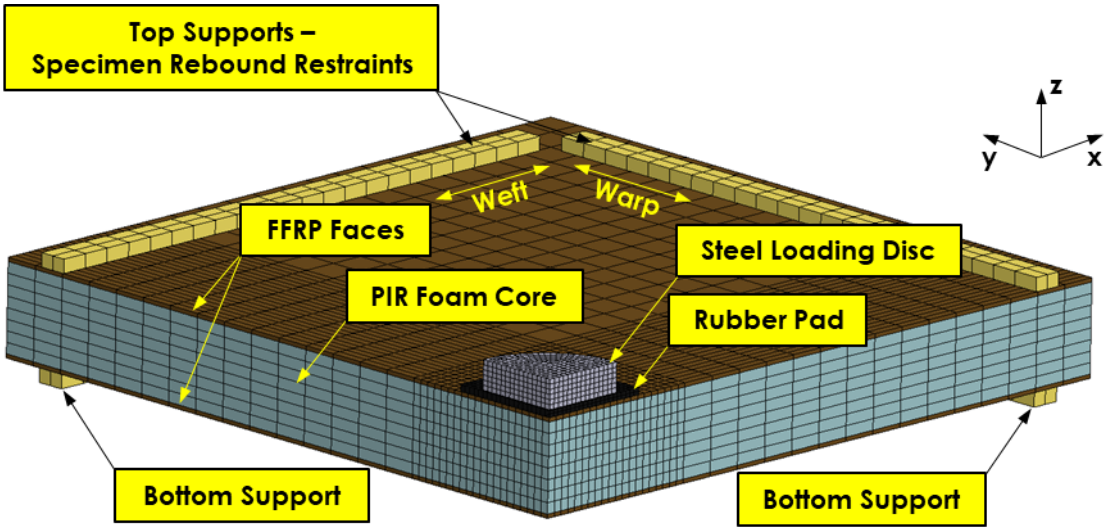

Figure 10. Impact FE model of sandwich panels with FFRP faces and foam cores

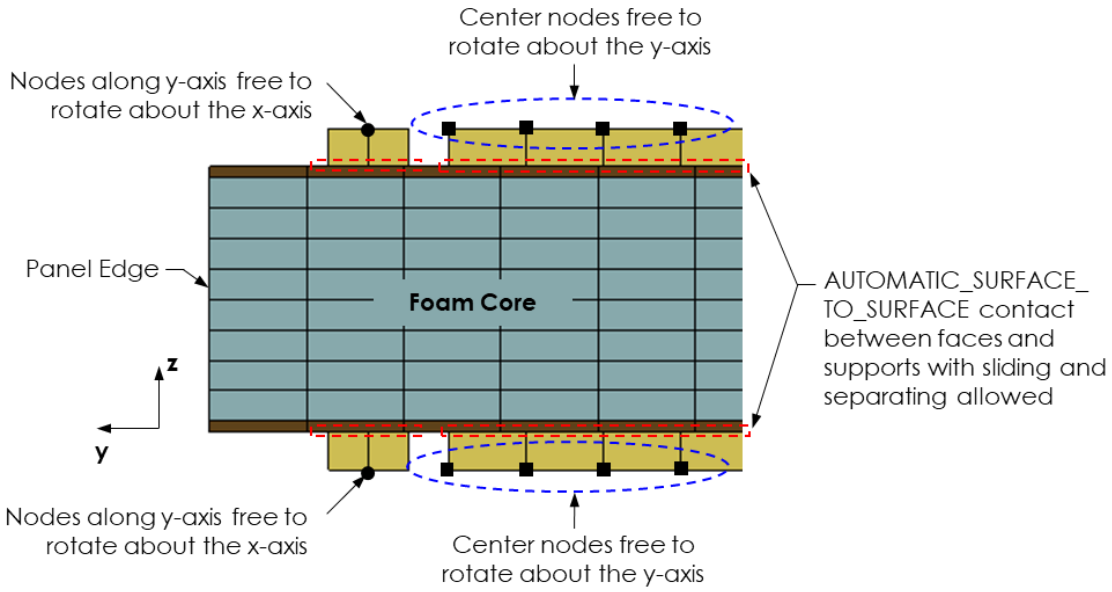

Figure 11. Modelling of panel supports in impact FE model

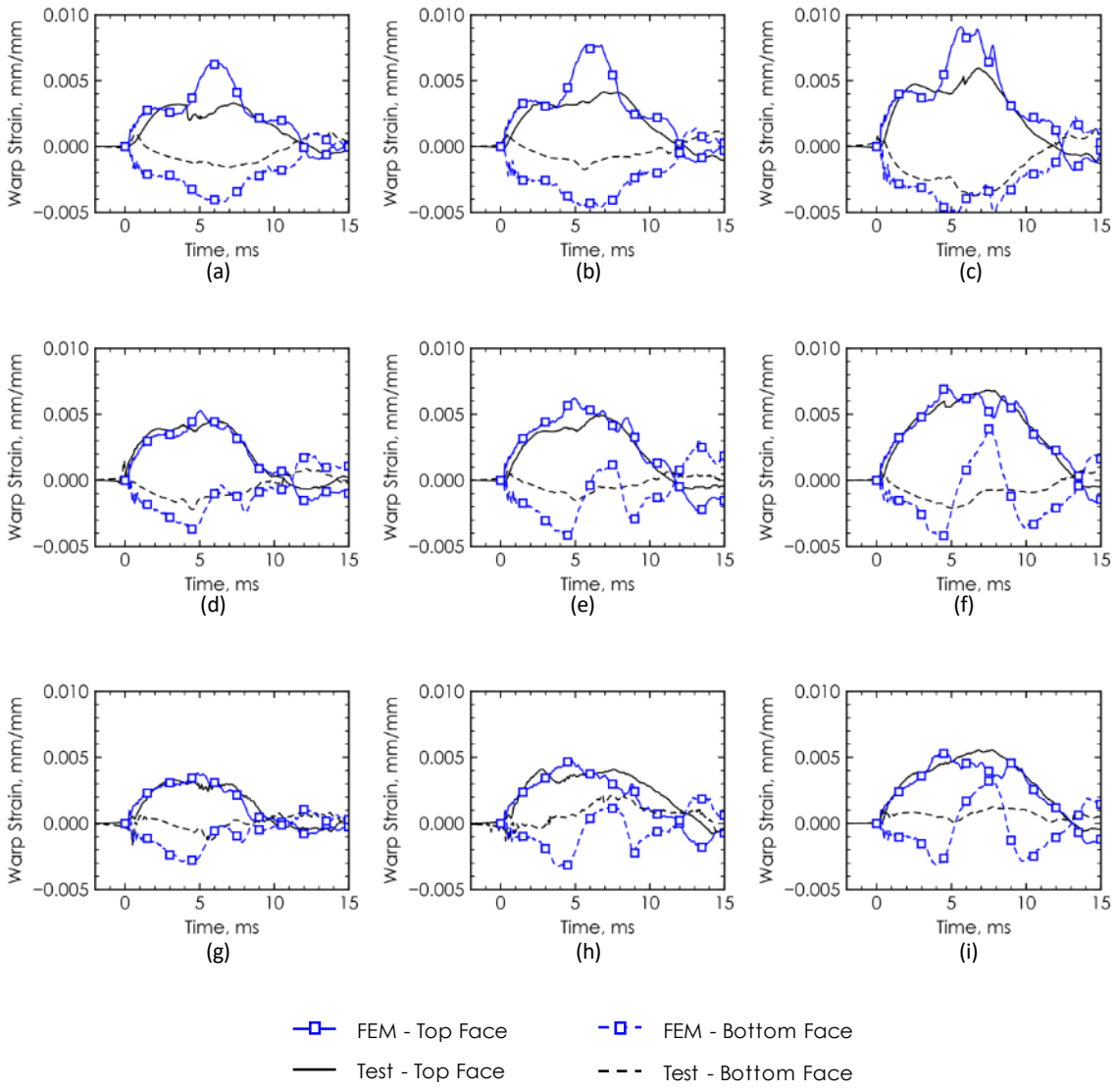

Figure 12. Impact FE model verification for 1FL panel at (a) 50% static failure energy (SFE); (b) 70% SFE and (c) 95% SFE, for the 2FL panel at (d) 50% SFE; (e) 70% SFE and (f) 95% SFE and for the 3FL panel at (g) 50% SFE; (h) 70% SFE and (i) 95% SFE

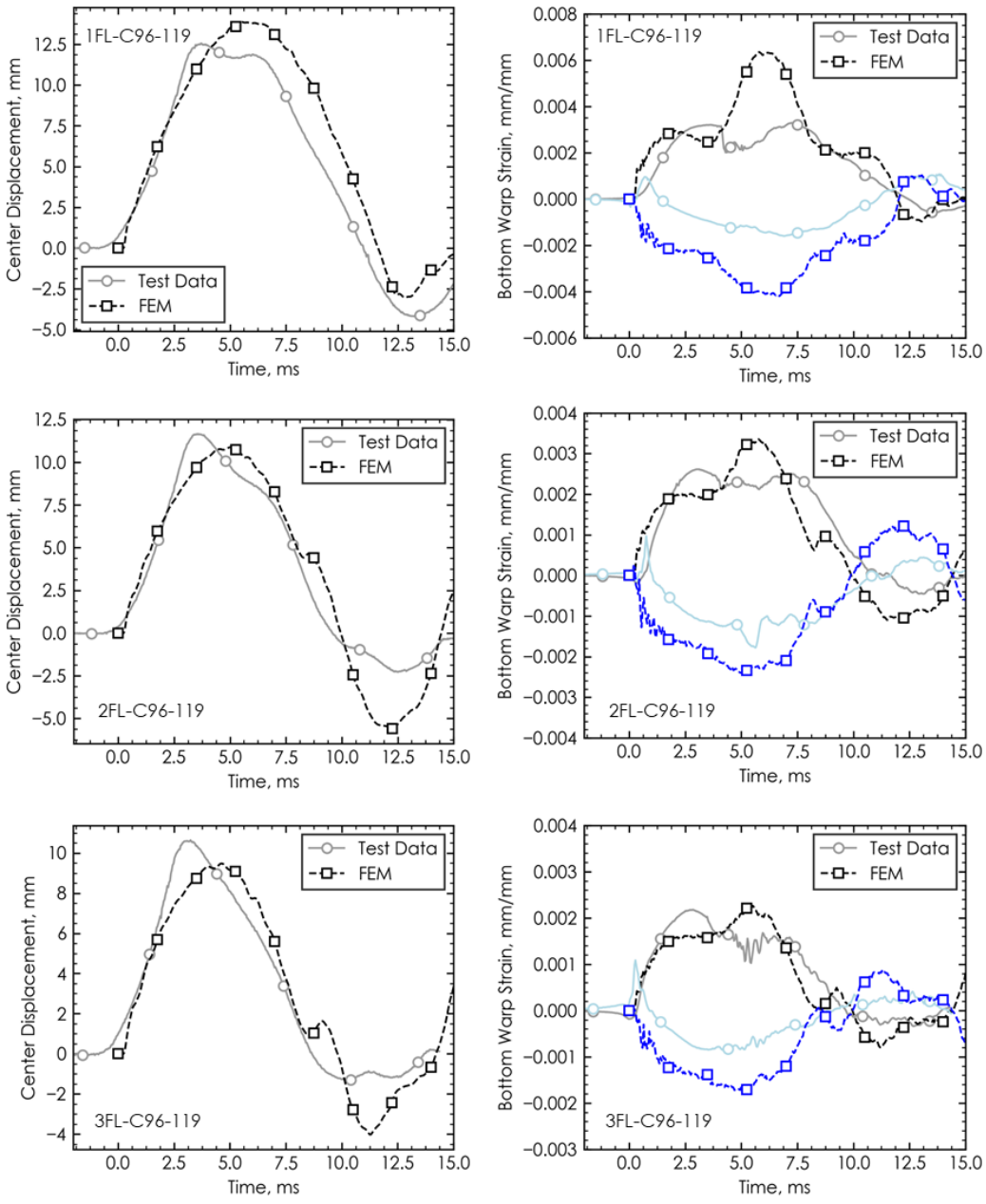

Figure 13. FE model verification for two-way sandwich panels subjected to 119 J impacts

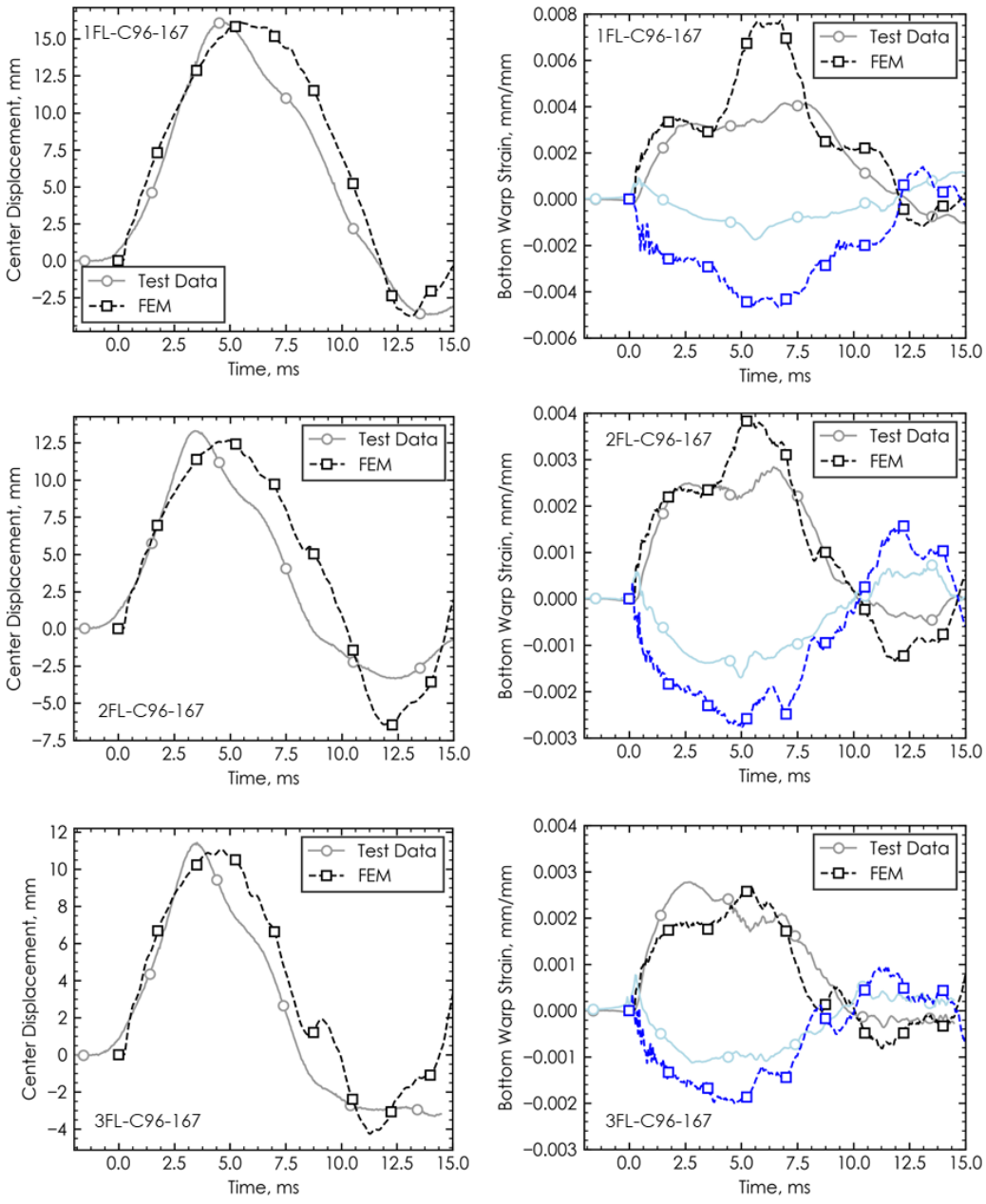

Figure 14. FE model verification for two-way sandwich panels subjected to 167 J impacts

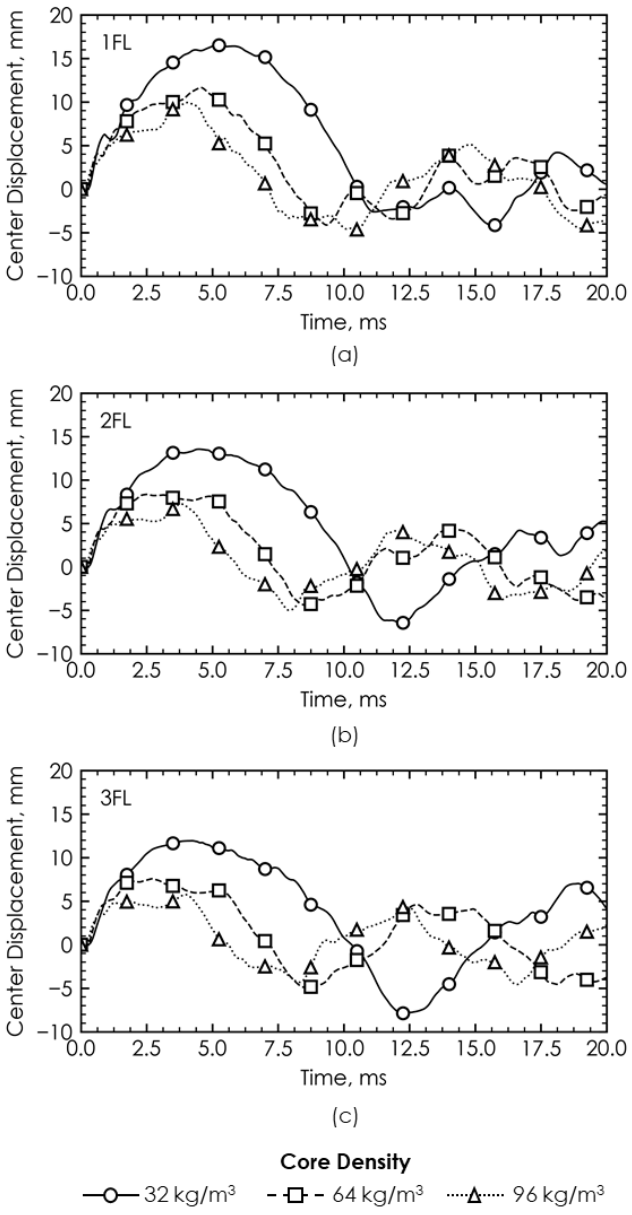

Figure 15. Effect of core density on the center displacement response of sandwich panels subjected to an 80 J impact (a) 1FL; (b) 2FL; and (c) 3FL [Note downward displacement is shown as positive]

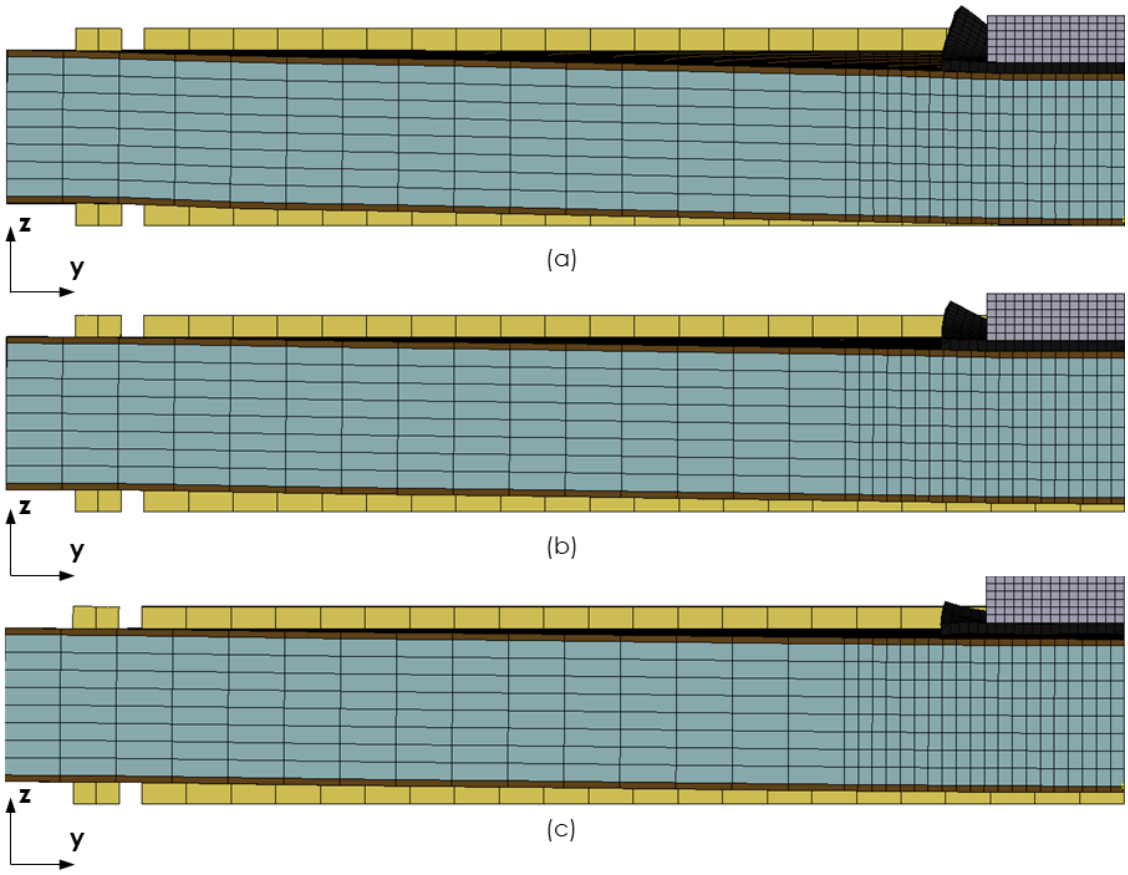

Figure 16. Maximum downward displacement shapes of panels (a) 1FL-C32; (b) 2FL-C32; and (c) 3FL-C32

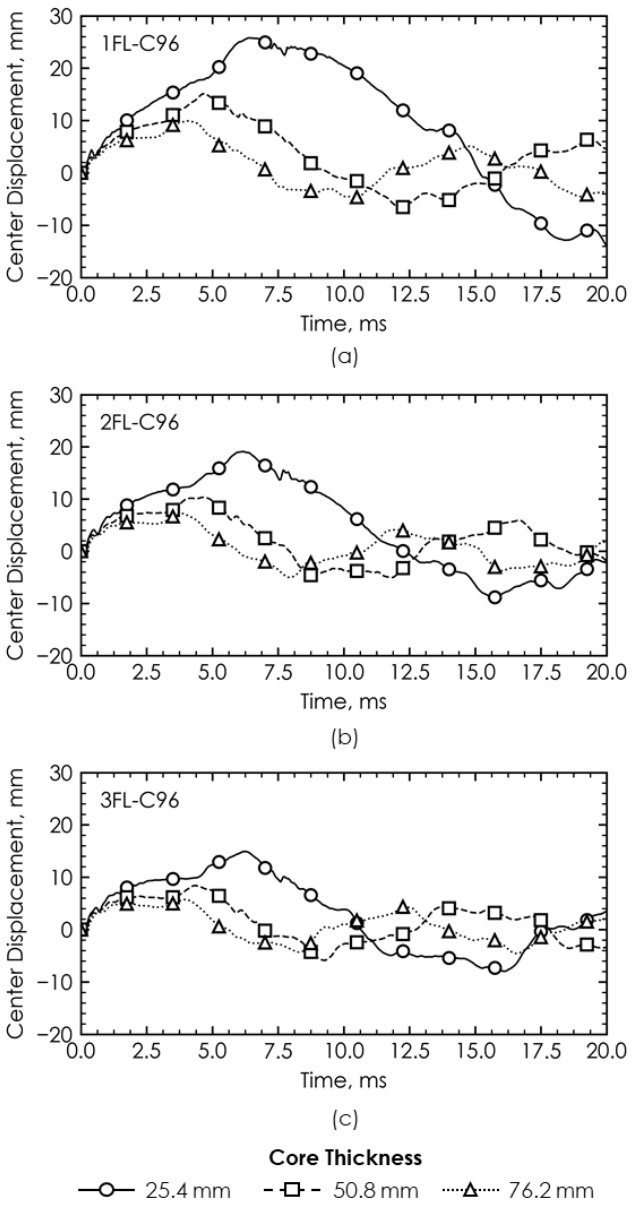

Figure 17. Effect of core thickness on the center displacement response of sandwich panels subjected to an 80 J impact (a) 1FL-C96; (b) 2FL-C96; and (c) 3FL-C96 [Note downward displacement is shown as positive]